# Anisotropic properties of periodically polarity-inverted zinc oxide structures

J. S. Park,[1,2] T. Minegishi,[1] J. W. Lee,[3] S. K. Hong,[4] J. H. Song,[5] J. Y. Lee,[3] E. Yoon,[2,a)] and T. Yao[1,b)]

[1]*Center for Interdisciplinary Research, Tohoku University, Sendai 980-8578, Japan*
[2]*Department of Materials Science and Engineering, WCU Hybrid Materials Program, Seoul National University, Seoul 151-742, South Korea*
[3]*Department of Material Science and Engineering, KAIST, Daejeon 305-701, South Korea*
[4]*Department of Materials Science and Engineering, Chungnam National University, Daejeon 305-764, South Korea*
[5]*Department of Physics, Kongju National University, Chungnam 314-701, South Korea*

(Received 24 February 2010; accepted 27 April 2010; published online 22 June 2010)

We report on the anisotropic structural properties of periodically polarity-inverted (PPI) ZnO structures grown on patterned templates. The etching and growth rates along $\langle 11\bar{2}0\rangle$ direction of ZnO structures are higher than those of $\langle 10\bar{1}0\rangle$ direction of ZnO films. From the strain evaluation by Raman spectroscopy, compressive strains are observed in all PPI ZnO samples with different stripe pattern size and the smaller pattern size is more effective to residual stress relaxation. The detailed structures at transition region show relationship with the anisotropic crystal quality. © *2010 American Institute of Physics*. [doi:10.1063/1.3436575]

## I. INTRODUCTION

Zinc oxide (ZnO) is a representative wide band gap compound semiconductor with a large exciton binding energy (60 meV) and piezoelectric constant.[1,2] The unique properties have made it as the most promising candidate material for a wide variety of applications in the fields of optoelectronics, transparent conduction electrodes, spintronics, and gas sensors.[3–5] Recently, the manipulation of growth kinetics using the anisotropic growth characteristics of ZnO materials is considered as a useful method to change the growth behaviors of ZnO.[6] The surface energy for $(1\bar{1}00)$ and $(11\bar{2}0)$ plane was calculated 0.91 $\mathrm{J/m^2}$ and 1.64 $\mathrm{J/m^2}$, respectively, which can be an origin of anisotropic crystal growth.[7]

Although there have been significant research for the growth and properties of ZnO nanostructures,[6,8] few studies to understand material properties related with the anisotropic growth behaviors have been conducted for the thin films.[9] In particular, the patterning and regrowth techniques are considered as the advanced and useful techniques to control the growth of micro- and nanostructured material systems.[10,11]

The attempts for periodical array of ZnO structures consisting of Zn-polar and O-polar on patterned template were reported in articles to extend application fields to nonlinear optics.[12,13] Recently, we demonstrated the second harmonic generation using the periodically polarity-inverted (PPI) ZnO structures.[14] Therefore, the proper understanding of this interesting growth behavior depending on the direction of patterned templates will be the first step to understand how to control the material properties.

In this work, we report on the anisotropic growth of ZnO heterostructures depending on the direction of etched templates and its detailed effects on materials properties.

## II. EXPERIMENTAL DETAILS

The one-dimensional (1D) PPI ZnO structures were fabricated on c-sapphire substrates by plasma assisted molecular beam epitaxy (PA MBE), where the growth and patterning sequences were obtained by carrying out photolithography and regrowth, as illustrated in Fig. 1. A 5 nm thick CrN layer is grown on (0001) $Al_2O_3$ by PA MBE. First, low-temperature (LT) ZnO layers are grown on a Zn-exposed

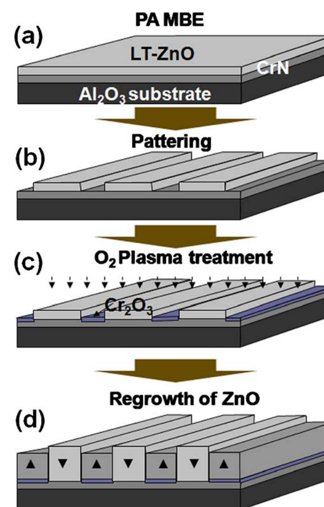


FIG. 1. (Color online) Schematic illustration of overall processes for PPI ZnO fabrication. (a) LT-ZnO growth on the Zn pre-exposed CrN buffer. (b) Formation of stripe patterns on the LT-ZnO along $\langle 11\bar{2}0\rangle$ and $\langle 10\bar{1}0\rangle$ direction. (c) O-plasma treatment on 1D patterned ZnO/CrN after chemical etching.(d) HT-ZnO growth.

a)Electronic mail: eyoon@snu.ac.kr. Tel.:+82 −2- 880- 7169. FAX: +82- 2-6008- 3712.
b)Electronic mail: tyao@cir.tohoku.ac.jp. Tel.:+81-22-795-4404. FAX: +81-22-795-2867.

 © 2010 American Institute of Physics

Downloaded 11 Apr 2011 to 143.248.103.56. Redistribution subject to AIP license or copyright; see http://jap.aip.org/about/rights_and_permissions

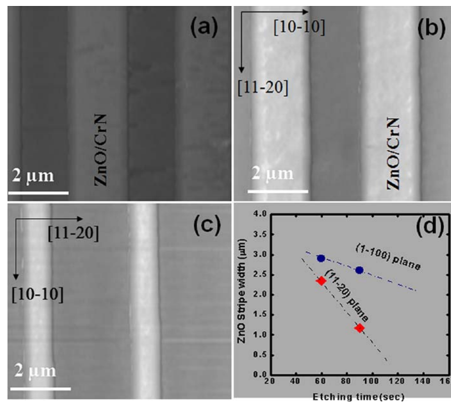


FIG. 2. (Color online) AFM images of etched ZnO structures. (a) Etched ZnO/CrN surface after 1 min. (b) etched ZnO/CrN stripe patterned direction $[11\bar{2}0]$ and (c) $[10\bar{1}0]$ direction for more 30 s, respectively. (d) Etching rate dependence on the pattern directions.

$CrN/Al_2O_3$ which can protect CrN surface from oxidation.[12] The polarity of LT-ZnO grown on CrN is Zn-polar with epitaxial relationship between ZnO and CrN as $ZnO(0001)\parallel CrN(111)$ and $ZnO(2\bar{1}\bar{1}0)\parallel CrN(01\bar{1})$.[12] Next, 1D periodic stripes have patterned on the LT-ZnO. The stripe pattern size (width of one stripe pattern) is changed from the 2 to 30 $\mu$m. Moreover, the stripe directions are changed $[11\bar{2}0]$ A-direction and $[10\bar{1}0]$ M-direction of ZnO films. After these patterns are obtained, the LT-ZnO layers are completely etched by the mixture of ethylenediaminetetraacetic acid and ethylenediamine solution (EDTA:ED=20:1) at room temperature. For the formation of a $Cr_2O_3$ layer, O-plasma treatment was conducted onto the exposed CrN surface; this led to the formation of $Cr_2O_3$ layers on CrN surface in patterns shown in Fig. 1(c); the formation of $Cr_2O_3$ is essential for the subsequent growth of O-polar ZnO film. Finally, a high-temperature (HT) ZnO layer was grown on the LT-ZnO; this results in the growth of the Zn-polar ZnO on the CrN area and the O-polar ZnO on the $Cr_2O_3/CrN$ area.[12] The polarity control and lateral polarity determination of ZnO hetero structures used in this work can be found out in other articles.[12,13] In order to measure the lateral growth rate depending on the etched facet direction of ZnO, the atomic force microscopy (AFM) measurement was conducted before and after the etching and regrowth, respectively. After the fabrication of 1D PPI ZnO structures, the behavior of strain relaxation and crystal quality are investigated by the micro-Raman ($\mu$-Raman) spectroscopy, photoluminescence (PL), and high resolution x-ray diffraction (XRD). The detailed microstructures are investigated using the high resolution transmission electron microscopy (HRTEM).

## III. RESULTS AND DISCUSSION

In order to get an insight into the etching and growth behaviors of ZnO films grown on patterned templates, the lateral direction etching rates are calculated by measurement of change in width of ZnO stripe during etching process. In Fig. 2, the etched surface of LT-ZnO film after etching for 1 and 1.5 min are shown with different stripe direction along with A-planes (b) and M-planes (c), respectively. The results clearly show the different etching rate depending on the patterned stripe direction. The etching rate of A-direction is 15.36 nm/min and that of M-direction is 9.89 nm/min as shown in Fig. 2(d). Recently Palacios-Lidón *et al.*[15] reported the different etching behaviors in 0.01 mol HCl[aq] along the miller indices crystallographic planes in ZnO based on the polarity and dangling bond of oxygen. In terms of surface density of oxygen dangling bonds per $nm^2$, the $\{10\bar{1}0\}$ and $\{11\bar{2}0\}$ plane show 5.9 and 6.8, respectively. The high dangling bonds seek more easily the etchant which makes more fast etching rate. Although the etching solution used in Ref. 15 is different from our experimental, the etching behaviors are well agreed with our experimental results. Moreover, the lateral direction growth rates of ZnO are also measured after growth of PPI ZnO structures on patterned templates. As expected in etching rate, the growth rate along the A-direction shows the 3.32 nm/min which is 1.37 times higher than that of M-direction.

To help intuitional understanding of etching characteristics depending on the planes of ZnO material in detail, atomic packing density of plane is considered. Figures 3(a) and 3(b) show the surface atomic configurations of ZnO $(10\bar{1}0)$ and $(11\bar{2}0)$ planes, respectively. The atomic packing density of plane has strong relationship with the etching rate i.e., the denser atomic packing density makes the slower etching and *vice versa*.[16] The atomic packing density is very higher in $\{10\bar{1}0\}$ plane when compared to the $\{11\bar{2}0\}$ plane as shown in Fig. 3. From this information we can expect that the etching rate and growth rate should be faster in A-direction than in M-direction. This consideration is well agreed with the theoretical expectation and experimental results. The theoretical calculation values of surface energy

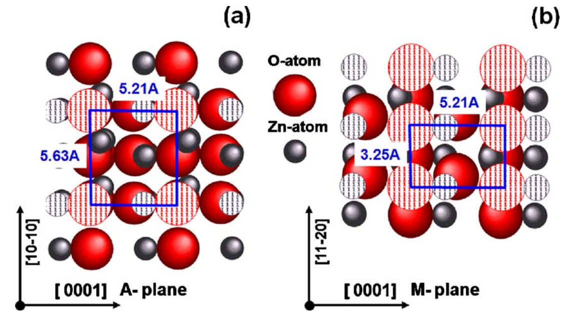


FIG. 3. (Color online) Surface atomic arrangement of (a) $(11\bar{2}0)$ ZnO and (b) $(10\bar{1}0)$ ZnO, respectively

TABLE I. Summary of the surface energy, etching rate, and growth rate depending on the plane of ZnO.

| Plane of ZnO | Surface energy[a] ($J/m^2$) | Etching rate (nm/min) | Growth rate (nm/min) |
|---|---|---|---|
| $(10\bar{1}0)$ | 0.96 | 9.9 | 2.42 |
| $(11\bar{2}0)$ | 1.64 | 15.4 | 3.32 |
| (0001) | 1.74 | 15.0 | 5.83 |
| $(000\bar{1})$ | | 142.5 | 4.53 |

[a]Reference 7.

Downloaded 11 Apr 2011 to 143.248.103.56. Redistribution subject to AIP license or copyright; see http://jap.aip.org/about/rights_and_permissions

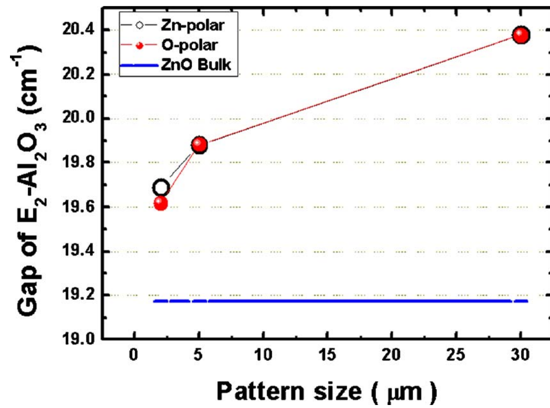


FIG. 4. (Color online) (Color online) Raman $E_2$ (high) mode shift as a function of pattern size. The black open circle and red ball show the Zn-polar and O-polar regions, respectively. In order to take reference, bulk ZnO is used (blue line).

depending on various planes of ZnO (Ref. 7) and experimental results in this study about the lateral growth rates and etching rates are summarized in Table I.

In order to evaluate the residual strain in PPI ZnO heterostructures, $\mu$-Raman spectroscopy measurements are carried out using a LabRam HR-UV/Vis/NIR (HORIBA Jobin Yvon) with a 0.4 $cm^{-1}$ spectral resolution.

Figure 4 shows the peak position gap between $E_2$ (high) mode peak and sapphire substrate obtained from the Raman spectra of the ZnO films with different stripe pattern size. The wave numbers of sapphire mode and $E_2$ mode of ZnO are determined as 417 $cm^{-1}$ and 438 $cm^{-1}$, respectively.[17,18] Because the $E_2$ (high) mode of Raman peak shift gives information about the stress in wurtzite structure, it is usually used to analyze the stress in epitaxial films. The Raman signal of ZnO single crystal is obtained for reference signal of $E_2$ (high) mode.

Huang *et al.*[19] showed that an increase in the $E_2$ photon frequency was ascribed to compressive stress, whereas a decrease in the $E_2$ phonon frequency was ascribed to tensile stress. The $E_2$ (high) mode of stress-free bulk ZnO is obtained at 437 $cm^{-1}$. But it could shift in ZnO thin films due to the strain caused by lattice mismatch between ZnO and substrate. For the ZnO films grown on relatively wide striped pattern, the $E_2$ mode is up-shifted comparing to the narrow pattern size. This result indicates that the PPI ZnO film grown on the wider patterned templates suffers the more compressive stress.

In the epitaxial ZnO films directly grown on $Al_2O_3$ (0001) substrate, the lattice constant of ZnO film is larger than that of the substrate at the growth temperature, which induces a large compressive misfit strain in the ZnO films.[20] As the lateral pattern size decreases, the residual strain in ZnO films reduced due to the relaxation of residual misfit compressive strain which means the narrow pattern size is more effective to relieve the stress. Moreover, the Raman frequency of Zn-polar and O-polar shows the same value which means the existence of same residual strain in both regions which are double checked by the micro-PL (not shown here).

In addition, PL measurement conducted at 10 K by using the He–Cd 325 nm excitation source. For the more detailed strain evaluation using the PL with a 0.5 $\mu$m spatial measurement resolution, a PPI ZnO with 500 nm stripe pattern size and bulk ZnO sample (Tokyo Denpa) are used. The incident laser beam impinged perpendicular to stripe pattern with 45° angle on surface and the emission was collected on surface of PPI ZnO. PL peaks are assigned $D^oX$, e-A, and longitudinal optical (LO) phonon replica peak as following the reference articles.[21] The PL spectra around band edge of ZnO heterostructures show the shift in emission peaks. Especially, the shift in e-A peak and phonon replica peaks are clearly shown. Unfortunately, it is difficult to define the shift in excitonic emission peaks in PPI ZnO with 500 nm pattern size due to the separation of dominant peak as shown in Fig. 5. The Fig. 5(b) clearly shows the blue shift in peak position with the increase in stripe pattern size. The shift toward higher energy indicates that the more compressive stressed ZnO was grown on relatively wider patterns. The results obtained from PL measurements are consistent with those of the Raman analyses.

Figure 6 shows the change in full width at half maximum (FWHM) of XRD rocking curves of ZnO (0002) peak as a function of azimuthal angle $\varnothing$ which is the angle between the stripe direction and the rotation axis in $\omega$ scan for XRD measurements where, for $\varnothing=0°$ is incident x-ray per-

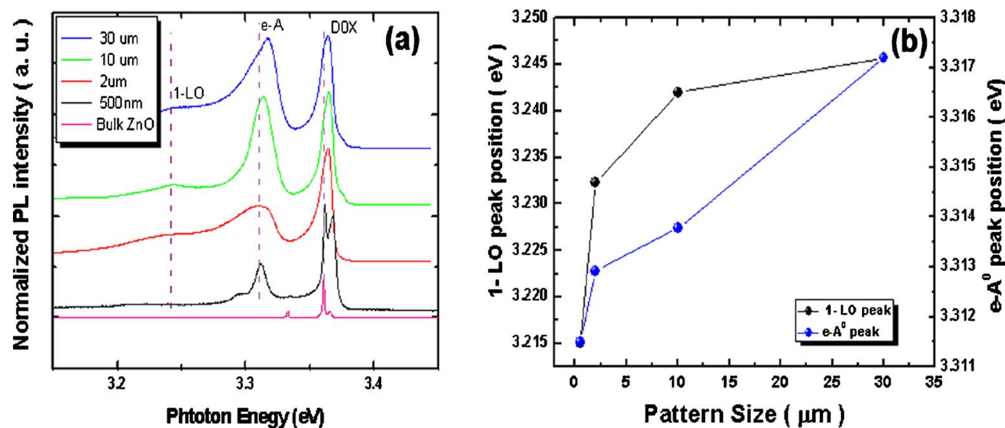


FIG. 5. (Color online) (a) PL spectra in 1D PPI ZnO structures with different pattern sizes and (b) peak shift as a function of pattern size. The peak assignment is denoted in figure.

Downloaded 11 Apr 2011 to 143.248.103.56. Redistribution subject to AIP license or copyright; see http://jap.aip.org/about/rights_and_permissions

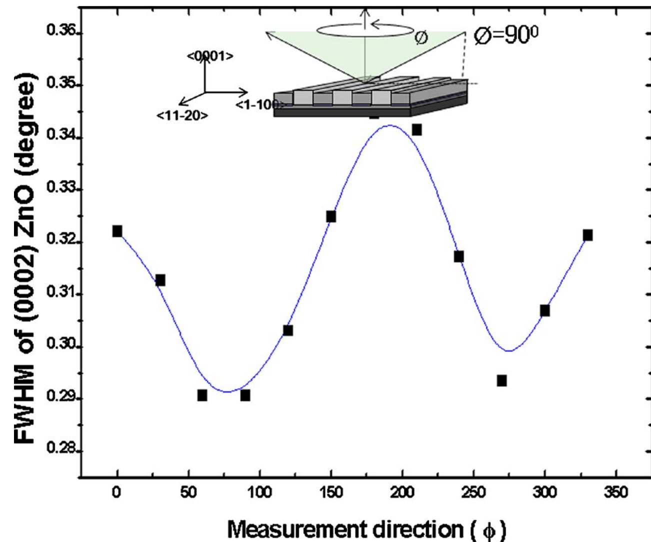


FIG. 6. (Color online) The change in FWHM of (0002) ZnO XRD rocking curves as a function of measured azimuthal angle. Inset shows the measurement methods.

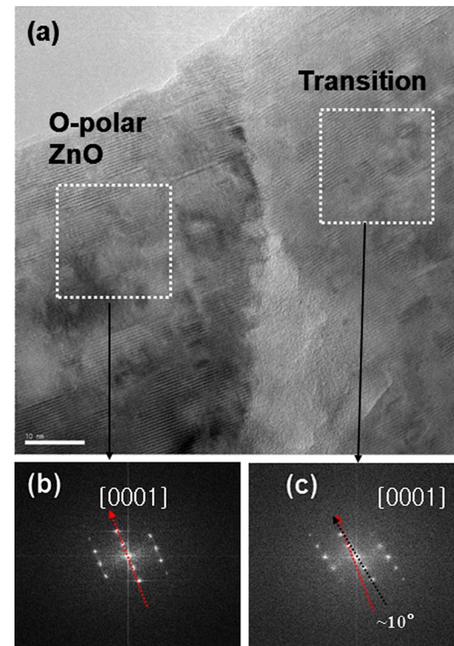


FIG. 7. (Color online) (a) HRTEM image obtained polar ZnO region and transition regions. (b) and (c) are the DDPs obtained marked region in (a).

pendicular to stripe and ∅=90° is parallel, respectively. The minimum and maximum values for FWHM of ZnO (0002) peak are periodically appeared with changing of azitmuthal ∅ angle. The parallel measurement direction along stripe pattern shows the narrower FWHM values comparing to perpendicular direction with pattern. In the case of lateral epitaxial overgrown GaN layers on $SiO_2$ mask, the FWHM broadening with change in measurement direction depends on strain anisotropy to thickness and lateral growth speed.[22,23] The anisotropy properties related to the anisotropic strain relaxation and tilted domain coming from the interface between films and mask. As following these previous reports, the anisotropic behaviors in PPI ZnO structures can be explained by the structural tilting or mixed planes in lateral growth direction coming from the different growth rates depending on the polarity, perpendicular to the stripe patterns.

In order to investigate the detailed microstructures between Zn-polar and O-polar region, the HRTEM images are obtained as shown in Fig. 7(a). Park *et al.*[24] reported the inversion domain boundary formation between both polar region in similar structured PPI ZnO structures. In this time, we want to focus on the transition regions to find out the origin of anisotropic broadening of FWHM of ZnO (0002). Digital diffraction patterns (DDPs) obtained by fast Fourier transformation of the HRTEM image are also shown in the Figs. 7(b) and 7(c). The DDPs are obtained from the marked white square regions on O-polar ZnO and transition region on the HRTEM image. The tilting about 10° between polar ZnO and transition regions are clearly shown as indicated red and black arrow on the DDPs. This tilted mosaicity can affect on the broadening of FWHM of ZnO (0002) which is similar to the tilting effects on the deterioration of crystal quality in GaN grown on masked region.[22]

## IV. SUMMARY

The effects of anisotropic growth characteristics in PPI ZnO grown on patterned templates with different pattern size and direction are investigated in detail. The etching and growth rates of $\langle 11\bar{2}0\rangle$ direction are about 1.5 and 1.3 times higher than those of $\langle 10\bar{1}0\rangle$ direction, respectively. The different dangling bond and atomic density depending on plane of ZnO were considered to explain these characteristics. The origin of anisotropic crystal quality in PPI ZnO might come from the mixed mosaicity in transition region between Zn-polar and O-polar regions. Moreover, the relatively narrow stripe pattern size shows effective compressive stress reduction by the strong relaxation which will help to control the strain and material properties.

## ACKNOWLEDGMENTS

This research was supported by WCU (World Class University) program through National Research Foundation of Korea funded by the Ministry of Education, Science and Technology (Grant No. R31-2008-000-10075-0).


[1] Ü. Özgür, Y. I. Alivov, C. Liu, A. Teke, M. A. Reshchikov, S. Dogan, V. Avruntin, S. J. Cho, and H. MorkoÇ, J. Appl. Phys. **98**, 041301 (2005).
[2] D. M. Bagnall, Y. F. Chen, Z. Zhu, S. Koyama, M. Y. Shen, T. Goto, and T. Yao, Appl. Phys. Lett. **70**, 2230 (1997).
[3] S. J. Jiao, Z. Z. Zhang, Y. M. Lu, D. Z. Shen, B. Yao, J. Y. Zhang, B. H. Li, D. X. Zhao, X. W. Fan, and Z. K. Tang, Appl. Phys. Lett. **88**, 031911 (2006).
[4] Q. Wan, Q. H. Li, Y. J. Chen, T. H. Wang, X. L. He, J. P. Li, and C. L. Lin, Appl. Phys. Lett. **84**, 3654 (2004).
[5] S. Polarz, A. Roy, M. Lehmann, M. Driess, F. E. Kruis, Z. Hoffmann, and P. Zimmer, Adv. Funct. Mater. **17**, 1385 (2007).
[6] X. Y. Kong, Y. Ding, R. Yang, and Z. L. Wang, Science **303**, 1348 (2004).
[7] M. Kim, Y. J. Hong, J. Yoo, G.-C. Yi, G.-S. Park, K. J. Kong, and H. Chang, Phys. Status Solidi (RRL) **2**, 197 (2008).
[8] L. E. Greene, M. Law, D. H. Tan, M. Montano, J. Goldberger, G. Somorjai, and P. Yang, Nano Lett. **5**, 1231 (2005).
[9] D. Andeen, J. H. Kim, F. F. Lange, G. K. Goh, and S. Tripathy, Adv. Funct. Mater. **16**, 799 (2006).
[10] O. Parillaud, E. Gil-Lafon, B. Gérard, P. Etienne, and D. Pribat, Appl. Phys. Lett. **68**, 2654 (1996).


Downloaded 11 Apr 2011 to 143.248.103.56. Redistribution subject to AIP license or copyright; see http://jap.aip.org/about/rights_and_permissions

[11]H. Marchand, X. H. Wu, J. P. Ibbetson, P. T. Fini, P. Kozodoy, S. Keller, J. S. Speck, S. P. DenBaars, and U. K. Mishra, Appl. Phys. Lett. **73**, 747 (1998).
[12]J. S. Park, S. K. Hong, T. Minegishi, S. H. Park, I. H. Im, T. Hanada, M. W. Cho, and T. Yao, Appl. Phys. Lett. **90**, 201907 (2007).
[13]J. S. Park, T. Minegishi, S. H. Lee, I. H. Im, S. H. Park, T. Hanada, T. Goto, M. W. Cho, T. Yao, S. K. Hong, and J. H. Chang, J. Vac. Sci. Technol. A **26**, 90 (2008).
[14]J. S. Park, Y. Yamazaki, I. Masanobu, S. Ahn, H. Jeon, T. Fujiwara, and T. Yao, Opt. Express **18**, 7851 (2010).
[15]E. Palacios-Lidón, B. Pérez-Gardica, P. Vennéguès, J. Colchero, V. Muñoz-Sanjosé, and J. Zúñiga-Pérez, Nanotechnology **20**, 065701 (2009).
[16]K. E. Bean, IEEE Trans. Electron Devices **25**, 1185 (1978).
[17]C. Bundesmann, N. Ashkenov, M. Schubert, D. Spemann, T. Butz, E. M. Kaidashev, M. Lorenz, and M. Grundmann, Appl. Phys. Lett. **83**, 1974 (2003).
[18]G. W. Cong, H. Y. Wei, P. F. Zhang, W. Q. Peng, J. J. Wu, X. L. Liu, C. M. Jiao, W. G. Hu, Q. S. Zhu, and Z. G. Wang, Appl. Phys. Lett. **87**, 231903 (2005).
[19]Y. Huang, M. Liu, Z. Li, Y. Zeng, and S. Liu, Mater. Sci. Eng., B **97**, 111 (2003).
[20]Y. Chen, D. M. Bagnall, H.-J. Ko, K.-T. Park, K. Hiraga, Z. Zhu, and T. Yao, J. Appl. Phys. **84**, 3912 (1998).
[21]B. K. Meyer, H. Alves, D. M. Hofmann, W. Kriegseis, D. Forster, F. Bertram, J. Christen, A. Hofmann, M. Straßburg, M. Dworzak, U. Haboeck, and A. V. Rodina, Phys. Status Solidi B **241**, 231 (2004).
[22]P. Fini, A. Munkholm, C. Thompson, G. B. Stephenson, J. A. Eastman, M. V. Ramana Murty, O. Auciello, L. Zhao, S. P. DenBaars, and J. S. Speck, Appl. Phys. Lett. **76**, 3893 (2000).
[23]M. H. Kim, Y. Choi, M. Yang, J. Jeon, S. Khym, and S. J. Leem, Appl. Phys. Lett. **79**, 1619 (2001).
[24]J. S. Park, T. Goto, S. K. Hong, S. H. Lee, J. W. Lee, T. Minegishi, S. H. Park, J. H. Chang, D. C. Oh, J. Y. Lee, and T. Yao, Appl. Phys. Lett. **94**, 141904 (2009).

**Downloaded 11 Apr 2011 to 143.248.103.56. Redistribution subject to AIP license or copyright; see http://jap.aip.org/about/rights_and_permissions**